Tree Physiology 0, 1–16
doi:10.1093/treephys/tpq086

Nitric oxide enhances salt secretion and Na^+ sequestration in a mangrove plant, *Avicennia marina*, through increasing the expression of H^+-ATPase and Na^+/H^+ antiporter under high salinity

JUAN CHEN,[1] QIANG XIAO,[2,1] FEIHUA WU,[1,5] XUEJUN DONG,[3] JUNXIAN HE,[4] ZHENMING PEI[5,1] and HAILEI ZHENG[1,6]

[1] *Key Laboratory for Subtropical Wetland Ecosystem Research of MOE, School of Life Sciences, Xiamen University, Xiamen 361005, People's Republic of China*

[2] *Laboratory of Biological Resources Protection and Utilization of Hubei Province, Hubei Institutes for Nationalities, Enshi 445000, People's Republic of China*

[3] *Central Grasslands Research Extension Center, North Dakota State University, Streeter, ND 58483, USA*

[4] *Institute of Plant Molecular Biology and Agricultural Biotechnology, The Chinese University of Hong Kong, Shatin, Hong Kong, SAR, China*

[5] *Department of Biology, Duke University, Durham, NC 27708, USA*

[6] *Corresponding author (zhenghl@xmu.edu.cn)*

Received May 31, 2010; accepted August 29, 2010; handling Editor Torgny Näsholm

Summary Modulation of nitric oxide (NO) on ion homeostasis, by enhancing salt secretion in the salt glands and Na^+ sequestration into the vacuoles, was investigated in a salt-secreting mangrove tree, *Avicennia marina* (Forsk.) Vierh. The major results are as follows: (i) under 400 mM NaCl treatment, the application of 100 μM sodium nitroprusside (SNP), an NO donor, significantly increased the density of salt crystals and salt secretion rate of the leaves, along with maintaining a low Na^+ to K^+ ratio in the leaves. (ii) The measurement of element contents by X-ray microanalysis in the epidermis and transversal sections of *A. marina* leaves revealed that SNP (100 μM) significantly increased the accumulation of Na^+ in the epidermis and hypodermal cells, particularly the Na^+ to K^+ ratio in the salt glands, but no such effects were observed in the mesophyll cells. (iii) Using non-invasive micro-test technology (NMT), both long-term SNP (100 μM) and transient SNP (30 μM) treatments significantly increased net Na^+ efflux in the salt glands. On the contrary, NO synthesis inhibitors and scavenger reversed the effects of NO on Na^+ flux. These results indicate that NO enhanced salt secretion by increasing net Na^+ efflux in the salt glands. (iv) Western blot analysis demonstrated that 100 μM SNP stimulated protein expressions of plasma membrane (PM) H^+-ATPase and vacuolar membrane Na^+/H^+ antiporter. (v) To further clarify the molecular mechanism of the effects of NO on enhancing salt secretion and Na^+ sequestration, partial cDNA fragments of PM H^+-ATPase (*HA1*), PM Na^+/H^+ antiporter (*SOS1*) and vacuolar Na^+/H^+ antiporter (*NHX1*) were isolated and transcriptional expression of *HA1*, *SOS1*, *NHX1* and vacuolar H^+-ATPase subunit c (*VHA-c1*) genes were analyzed using real-time quantitative polymerase chain reaction. The relative transcript abundance of the four genes were markedly increased in 100 μM SNP-treated *A. marina*. Moreover, the increase was reversed by NO synthesis inhibitors and scavenger. Taken together, our results strongly suggest that NO functions as a signal in salt resistance of *A. marina* by enhancing salt secretion and Na^+ sequestration, which depend on the increased expression of the H^+-ATPase and Na^+/H^+ antiporter.

Keywords: ion homeostasis, non-invasive micro-test technology (NMT), salt crystal, sodium nitroprusside (SNP), X-ray microanalysis.

Introduction

Soil salinity is a serious threat to agricultural production in limiting plant growth and productivity worldwide (Rengasamy 2006). Salt stress disturbs the intracellular ion homeostasis of plants, which leads to adverse effects on cytosolic enzyme activities, photosynthesis and metabolism (Hasegawa et al. 2000). Under salinity conditions, intracellular Na^+ to K^+ homeostasis is crucial for cell metabolism and is considered to be a strategy commonly used by tolerant plants (Chinnusamy et al. 2005). To maintain an optimal Na^+ to K^+ ratio in the cytosol, plants remove excess Na^+ through Na^+ extrusion to the external environment and/or compartmentalization into the vacuoles, along with retention of physiological K^+ concentration in the cytoplasm (Olias et al. 2009).

Active Na^+ extrusion from the cytosol is typically carried out by transmembrane transport proteins such as plasma membrane (PM)-located Na^+/H^+ antiporters and vacuolar membrane-located Na^+/H^+ antiporters (Shi and Zhu 2002, Xue et al. 2004, Yang et al. 2009, Oh et al. 2010), which are energy dependent and driven by the electrochemical gradient created by PM H^+-ATPase (PM H^+-ATPase) and by vacuolar membrane H^+-ATPase (V-H^+-ATPase) and H^+-pyrophosphatase (V-H^+-PPase) (Rea and Poole 1985, 1993, Chen et al. 2007, Silva et al. 2010).

The PM Na^+/H^+ antiporter is encoded by the salt overly sensitive-1 (*SOS1*) gene, which is described to be crucial for ion homeostasis and salt tolerance in plants (Zhu 2002, 2003). In *Arabidopsis thaliana*, PM-localized SOS1 functions as an Na^+/H^+ antiporter to extrude excess Na^+ from the cytosol and the defective phenotypes of *AtSOS1* plants suggest that Na^+ efflux is dominated by SOS1 (Shi et al. 2003). Generally, the expression of the *SOS1* gene is very low or undetectable under saltless condition and appears primarily in the root meristem zone and in parenchyma cells surrounding the vascular tissues in response to NaCl treatment (Shi and Zhu 2002). Therefore, *SOS1* has been suggested to be involved in long-distance Na^+ transport and in Na^+ extrusion from the root meristem zone into the surrounding medium under salt stress. Another member of the family of Na^+/H^+ antiporters to which *SOS1* belongs is the *NHX1* family (Quintero et al. 2000, 2002). In *Arabidopsis*, a vacuolar Na^+/H^+ antiporter (*AtNHX1*), a homolog of the yeast antiporter *NHX1*, was first cloned and functionally expressed in *Saccharomyces cerevisiae* (Gaxiola et al. 1999). Since then a series of Na^+/H^+ antiporter genes have been cloned and identified from *Oryza sativa* (Fukuda et al. 2004), *Mesembryanthemum crystallinum* (Chauhan et al. 2000), *Atriplex gmelini* (Hamada et al. 2001) and some other glycophytes and halophytes.

Compared with wild-type plants, Na^+ accumulated in *SOS1* or *NHX1* mutants increases in response to external NaCl concentration, at least in halophytic species (Blumwald 2000). Overexpression of *SOS1* or *NHX1* enhances salt tolerance by decreasing Na^+ accumulation in the cytoplasm of different transgenic plants such as *Arabidopsis*, *Lycopersicon esculentum* and *Brassica napus* (Apse et al. 1999, Zhang and Blumwald 2001, Shi et al. 2003). As the energy sources of Na^+/H^+ antiport, H^+ pumping in the PM and vacuolar membrane may represent a fundamental Na^+/H^+ exchange and salinity tolerance. Previous studies showed that PM H^+-ATPase activity was affected by salt treatment, including partial inhibition in *L. esculentum* (Kerkeb et al. 2001), stimulation in *Medicago citrine* (Sibole et al. 2005) and no effect in *Gossypium hirsutum* (Hassidim et al. 1986). Furthermore, salt treatment elevated the activity and the transcript level of subunits A and c of V-H^+-ATPase (Kirsch et al. 1996, Lehr et al. 1999). The up-regulation of V-H^+-ATPase activity is coordinated with Na^+/H^+ antiporter activity, which plays a pivotal role in sequestering Na^+ into the vacuoles (Chen et al. 2010).

Nitric oxide (NO) is an exceptional molecule due to the versatility of its actions in plant growth and development such as seed germination (Beligni and Lamattina 2002), stomatal closure (Neill et al. 2002), flowering repression (He et al. 2004), etc. NO can also mediate the plant's responses to biotic and abiotic stresses such as salt, heat, drought, UV-B and pathogen attack (Wendehenne et al. 2004, Malerba et al. 2008, Tossi et al. 2009, Zheng et al. 2009). It was reported that sodium nitroprusside (SNP), an exogenous NO donor, enhanced salt tolerance of plants by increasing dry matter accumulation, reducing oxidative damage and maintaining a lower cytoplasmic $Na^+$to K^+ ratio (Zhang et al. 2006, 2007, Shi et al. 2007). Zhang et al. (2006) reported that NO-stimulated H^+-ATPase produces an H^+ gradient across the vacuolar membrane, offering the force for Na^+/H^+ exchange which may contribute to Na^+ and K^+ homeostasis in plants. However, little is known about the precise mechanism of how the expression and regulation of the H^+-ATPases and Na^+/H^+ antiporters are affected by NO.

Avicennia marina (Forsk.) Vierh. is a mangrove tree that thrives in the tidal, saline wetlands along tropical and subtropical coasts (Duke et al. 1998). In order to cope with high salinity, *A. marina* has evolved a series of mechanisms to maintain osmotic balance and enhance salt tolerance, such as selective accumulation of ions, ion compartmentalization, salt secretion and accumulation or synthesis of compatible solutes (Parida and Jha 2010). The most peculiar characteristic of morphological and anatomical adaptations of salt-secreting mangrove plants is perhaps the development of salt glands that can prevent excess ion accumulation in leaves (Flowers et al. 1990). In many studies on the structure and function of salt glands in the *Avicennia* species, it has often been observed that the predominant cation secreted by salt glands is Na^+, which accounts for >93% of leaf secretion and is essential for sustaining ion homeostasis in the cytosol of cells (Drennan and Pammenter 1982, Boon and Allaway 1986, Sobrado and Greaves 2000, Sobrado 2001). In *A. marina* leaves, the number of salt glands increased with external salt concentrations and rates of salt secretion are enhanced greatly when plants are transferred to increasingly strong saline solutions (Drennan and Pammenter 1982, Boon and Allaway 1986, Ding et al. 2009). Furthermore, previous studies showed that various inhibitors, such as a proton pump inhibitor, a Ca^{2+} pump inhibitor and a K^+ channel inhibitor, affected salt secretion in the salt glands (Dschida et al. 1992, Balsamo et al. 1995). These studies establish that salt secretion is an energy-dependent process, achieved by some cation channels in concert with the electrochemical proton gradient generated by H^+ pumping (Balsamo et al. 1995). However, to the best of our knowledge, the mechanisms of NO-induced salt secretion by salt glands are not clear yet and alternations by NO have not been investigated.

In this study, various SNP concentrations were used to clarify the role that NO plays in maintaining lower Na^+ to K^+ ratio in the cytosol, thereby enhancing the salt tolerance

of *A. marina*. Our results show that an appropriate concentration of SNP induces increases in Na^+ secretion and net Na^+ efflux into salt glands, along with increased Na^+ sequestration into the vacuoles, through enhancing the translational and transcriptional expression of PM- and vacuolar membrane-located H^+-ATPase and Na^+/H^+ antiporter in the mangrove plant, *A. marina*.

Materials and methods

Plant materials and growth conditions

In September 2009, mature propagules of *A. marina* were collected from Zhangjiang River Estuary Mangrove National Nature Reserve (23°55′N, 117°26′E), Fujian Province, China. The collected propagules were similar in size and free from insect damage or fungal infection. They were planted in pots, each with a dimension of 40 cm (open top) × 30 cm (height) × 30 cm (flat bottom), and filled with clean sand. The propagules were cultivated in a greenhouse with a daily temperature of 25–28 °C, relative humidity of 60–70% and a 12-h photoperiod at 800–1000 µmol photons m^{-2} s^{-1} of photosynthetically active radiation. Plants were irrigated daily with tap water according to evaporation demand, and a full-strength Hoagland nutrient solution was added biweekly. Plants were raised for 2 months prior to the beginning of salt and SNP treatments.

Treatments

Plants of uniform size were transferred to individual pots and divided into two groups. The first group was supplied with a series of Hoagland nutrient solution containing various concentrations of NaCl (0, 100, 200, 400 and 600 mM). After 7, 30 and 40 days of salt treatment, the salt crystals on the surface of leaves were observed and photographed. In the second group, plants were supplied with SNP and NaCl for 30 days. Different amounts of SNP (0, 50, 100, 200, 500 µM) were added to the Hoagland nutrient solution containing 400 mM NaCl. The culture solution was replaced twice a week. The upper second leaves were carefully washed with distilled water in order to measure the salt secretion rate. The cation content of the washing solution and accumulated ionic fractions in leaves were determined later. Some plants were used immediately for Na^+ flux measurement, scanning electron microscopic observation, western blot and real-time quantitative polymerase chain reaction (PCR) analyses.

Fluorescent imaging of endogenous NO

Endogenous NO was visualized using the highly specific NO fluorescent probe 3-amino, 4-aminomethyl-2′,7′-difluorofluorescein diacetate (DAF-FM DA, Calbiochem), according to the method described by Corpas et al. (2006). Briefly, the slices and upper epidermis of *A. marina* leaf were incubated with 20 µM DAF-FM DA in 20 mM Tris–HCl (pH 7.4) for 2 h at 25 °C, in darkness. Then, the leaf slices and upper epidermis were washed three times using Tris–HCl buffer (pH 7.4) to wash off excess fluorophore. DAF-FM DA fluorescence was visualized using an inverted Motic AE31 fluorescence microscope (Speed Fair Co., Ltd, Hong Kong) with 480 nm excitation and 535 nm emission filters (Motic MHG-100B) (Speed Fair Co., Ltd, Hong Kong). Digital images were captured with a cool CCD camera controlled with Motic Image Advanced 3.2 software. At least six samples were measured in each treatment.

Ion analysis

To determine the cation content of the leaves, dried and ground leaves were placed into the digestion vessels, mixed with 5 ml of concentrated HNO_3 and digested in a microwave digestion system (CEM, Inc., Mars-V). The solution was finally diluted to a certain volume with deionized water. The cation content of leaf samples and leaf washing solutions were determined using inductively coupled plasma mass spectrometry (ICP-MS, PerkinElmer, Inc., Elan DRC-e).

X-ray microanalysis

Fresh leaves of *A. marina* were cut into 0.1 × 0.3 cm pieces and fixed for 24 h with 2.5% glutaraldehyde at room temperature. The materials were then washed with 0.1 M phosphate buffer solution (pH 7.0), fixed for 1.5 h with 1% OsO_4 and washed again with distilled water before being dehydrated in a series of concentrations of alcohol (50, 70, 80, 90, 95 and 100%) for 15 min. Isoamyl acetate was applied to infiltrate into the samples for 24 h, and then the samples were embedded and polymerized in the same isoamyl acetate for 24 h at 30, 45 and 60 °C. The materials were dried with a common critical point drier and platinized with an ion sputter (IB-5), and the samples were observed and photographed with a scanning electron microscope (SEM; JSM6390, JEOL, Kyoto, Japan) equipped with an energy dispersive X-ray detector (Kenex, Valencia, CA, USA) for element ratio measurements (Vazquez et al. 1999). At least 10 measuring regions on the abaxial surface, adaxial surface and transverse sections were examined. Each sample was examined within 10 min to avoid tissue distortion. The results were expressed as the percentage of the atomic number of a particular element (e.g., Na^+ and K^+) in the total atomic number for all elements measured (Na^+, K^+, Ca^{2+}, Mg^{2+}, Al^{3+}, Mn^{2+}) in a given measuring region.

Na^+ flux measurements

Net Na^+ fluxes in the salt glands of *A. marina* upper epidermis were measured noninvasively using non-invasive micro-test technology (NMT) by the BIO-IM NMT system

(Younger USA Sci. and Tech. Corp., Amherst, MA, USA) as described previously (Sun et al. 2009*a*, 2009*b*). Briefly, prepulled and silanized glass micropipettes (2–4 μm aperture, XY-Na-04; Xuyue Sci. and Tech. Corp., Ltd) were first filled with a backfilling solution (100 mM NaCl, pH 7.0) to a length of ~1 cm from the tip. Then the micropipettes were front filled with ~15-μm columns of selective liquid ion-exchange cocktails (LIXs; Sigma 71178). An Ag/AgCl wire electrode holder (XY-ER-01; Xuyue Sci. and Tech. Co., Ltd) was inserted in the back of the electrode to make electrical contact with the electrolyte solution. DRIREF-2 (World Precision Instruments, Inc., Sarasota, FL, USA) was used as the reference electrode. The electrode was moved in a predefined sampling routine (10 μm) by a three-dimensional microstepper motor manipulator (CMC-4). Prior to flux measurements, 0.5 and 5 mM NaCl were used to calibrate the ion-selective electrode. From the electrical recordings, Na^+ flux was calculated by Fick's law of diffusion, as described by Sun et al. (2009*a*), using MageFlux software (http://www.youngerusa.com/mageflux or http://xuyue.net/mageflux).

The upper epidermis of *A. marina* leaves was gently stripped, cut into 0.2 × 0.2 cm pieces, rinsed with redistilled water and immediately incubated in the measuring solution (0.1 mM KCl, 0.1 mM $CaCl_2$, 0.1 mM $MgCl_2$, 0.5 mM NaCl, 0.2 mM Na_2SO_4, 0.3 mM 2-(4-morpholino) ethanesulfonic acid, pH 6.0) to equilibrate for 30 min. Afterwards, the upper epidermis was immobilized on the bottom of a measuring chamber containing the fresh measuring solution (5–10 ml). Prior to Na^+ flux measurements, a salt gland could be found easily under the NMT microscope because the upper epidermis was semitransparent under light. The electrode was transferred to the proper position near the salt gland for net Na^+ flux measurement.

The effects of transient additions of SNP, NO synthesis inhibitors and PM H^+-ATPase and Na^+/H^+ antiporter inhibitors on Na^+ flux kinetics were examined in the salt glands of *A. marina*. Before the SNP or inhibitor addition, steady Na^+ flux was recorded for at least 10 min. Then an SNP or inhibitor was added to the measuring solution, with the transient Na^+ flux in the salt gland monitored for an additional 16–20 min. The data for the first 2–3 min were discarded due to the diffusion effects of SNP or inhibitor addition.

Sodium dodecyl sulfate–polyacrylamide gel electrophoresis and western blot analysis

Avicennia marina leaves (0.5 g) were ground in liquid nitrogen, and the crude protein extracts were solubilized in extraction buffer containing 50 mM phosphate-buffered saline (pH 7.5), 100 mM ethylenediaminetetraacetic acid, 1% polyvinylpyrrolidone (w/v), 1% Triton X-100 (v/v) and 2% β-mercaptoethanol (v/v). After centrifugation for 15 min (4 °C, 15,000 rpm), the upper phase was transferred to a new centrifuge tube. Two volumes of Tris-saturated phenol (pH 8.0) were added and then the mixture was further vortexed for 30 min. Proteins were precipitated by adding five volumes of ammonium sulfate-saturated methanol and incubated at −20 °C for at least 4 h. After centrifugation as described above, the protein pellets were re-suspended and rinsed with ice-cold methanol followed by ice-cold acetone twice, and spun down at 15,000 rpm for 5 min at 4 °C after each washing. Finally, the washed pellets were air-dried and recovered with lysis buffer containing 62.5 mM Tris–HCl (pH 6.8), 2% sodium dodecyl sulfate (v/v), 10% glycerol (v/v) and 2% β-mercaptoethanol (v/v). Protein concentrations were measured according to Bradford (1976).

Total protein (120 μg) was separated by 12% (w/v) standard sodium dodecyl sulfate–polyacrylamide gel electrophoresis (SDS–PAGE) and blotted to polyvinylidene fluoride membrane for 50 min. The membrane was blocked overnight with Western Blocking Buffer (TIANGEN, China). The protein blots were probed with a primary antibody. H^+-ATPase (AS07 260, Agrisera, Sweden) or Na^+/H^+ antiporter (AS09 484, Agrisera, Sweden) at a dilution of 1:2000 for 2 h at room temperature with agitation. Then the blot was washed three times in PBST solution (50 mM Tris–HCl, pH 8.0, 150 mM NaCl, 0.05% Tween 20, v/v), followed by incubation with the secondary antibody (anti-rabbit IgG horseradish peroxidase-conjugated; Abcam, UK, 1:5000 dilution) for 1 h at room temperature. The blots were finally washed as above and developed with SuperSignal® West Pico Chemiluminescent Substrate (Pierce, USA) according to the manufacturer's instructions. Images of the blots were obtained using a CCD imager (FluorSMax, Bio-Rad, Hercules, CA, USA) and protein signals were quantified using the Quantity One software (Bio-Rad).

RNA extraction and gene cloning

Total RNA was extracted from *A. marina* leaves using the TRIZOL reagents (Invitrogen, Inc., CA, USA) according to the manufacturer's instructions. Agarose gel electrophoresis and spectroscopy were used to confirm RNA integrity and quality. RNA was reverse transcribed to produce cDNAs using cloned AMV First-Strand cDNA synthesis kit (Invitrogen, Inc.), and the resulting cDNA mixture was used as templates for subsequent PCRs. Degenerate oligonucleotide primers corresponding to the highly conserved amino acid sequence of diverse genes obtained from GenBank were synthesized. The PCR to amplify the core fragment was performed with degenerate primers using Ex Taq™ HS DNA polymerase (Takara Bio, Inc., Japan) and 0.2 mM deoxy-ribonucleoside triphosphate in a final volume of 20 μl, according to the manufacturer's protocol.

For *HA1*, *SOS1* and *NHX1* genes, the reverse transcription products were partially amplified by reverse transcription-PCR (RT–PCR) using the degenerate primers and optimized reaction conditions as shown in Table 1. Amplified cDNA fragments derived from the *A. marina* genome were electrophoresed on a 1% agarose gel. On the basis of the predicted sizes of the amplified fragments,

Table 1. Optimized primer sequences and reaction conditions used for gene cloning and real-time quantitative PCR of *HA1*, *VHA-c1*, *SOS1*, *NHX1* and *18S* rRNA in *A. marina*.

Group and name	Primer sequences	Purpose	Optimized conditions (T_m/amplicon length)
HA1			
HA1 sense1	5′-AAGGCWGCHCAYCTBGTNGAYAGCAC-3′	Gene cloning	56.8 °C/508 bp
HA1 antisense1	5′-CCAGCHCKTGCCTCYTTNGGATCAG-3′	Gene cloning	
HA1 sense2	5′-TTGGTAACTTCTGTATTTGCTCCATTGCT-3′	qRT-PCR	60.0 °C/145 bp
HA1 antisense2	5′-AGTGGGCATAGCGATGGGAATACCTC-3′	qRT-PCR	
VHA-c1			
VHA-c1 sense	5′-CCTGATTATATGGTAGTTTGGCTGTGGA-3′	qRT-PCR	62.0 °C/217 bp
VHA-c1 antisense	5′-TACAGGCAACAGTTTTACACAAATCACAT-3′	qRT-PCR	
SOS1			
SOS1 sense1	5′-GAAGGGGAGTCGCTGATGAATGATGG-3′	Gene cloning	52.0 °C/1074 bp
SOS1 antisense1	5′-TTGDDKATYCKBCCCTCWTYRAGCAT-3′	Gene cloning	
SOS1 sense2	5′-GCTTTTGGAATAGCATCAGTCTTGTGGC-3′	qRT-PCR	60.0 °C/138 bp
SOS1 antisense2	5′-CCGTCAAAACTCCAGAAACATCAACTCCTT-3′	qRT-PCR	
NHX1			
NHX1 sense1	5′-ATHAARAAGYTTTACTTTGGMAGGCAC-3′	Gene cloning	52.0 °C/470 bp
NHX1 antisense1	5′-ACAGCTCCTCKCATRAGHCCAGCCCAC-3′	Gene cloning	
NHX1 sense2	5′-AGCATTCTTTCGCAACTTTGTCTTTCATT-3′	qRT-PCR	60.0 °C/112 bp
NHX1 antisense2	5′-CCAACAGATTTTCCAGGGCTTTTGCTTACA-3′	qRT-PCR	
18S rRNA			
18S rRNA sense	5′-ACGAACGAGACCTCAGCCTGCTAACT-3′	qRT-PCR	60.0 °C/114 bp
18S rRNA antisense	5′-CAGACCTGTTATTGCCTCAAACTTCC-3′	qRT-PCR	

T_m, annealing temperature.

the corresponding bands were purified with a membrane-mediated spin column (Takara Bio, Inc., Japan). The purified fragments were ligated to a plasmid vector of PMD-18T (Takara Bio. Inc.), introduced into *Escherichia coli*, and at least four identical clones of each gene were subjected to sequence analysis, using Vector NTI Advance™ 9.0 (Invitrogen, Inc.). Homology searches of gene and amino acid sequences were carried out by BLAST (http://blast.ncbi.nlm.nih.gov/). Partial sequences of *HA1*, *SOS1* and *NHX1* genes were acquired by aligning with known sequences (>70% homology) according to NCBI information (http://www.ncbi.nlm.nih.gov/). The sequences of *A. marina VHA-c1* and *18S* rRNA (GenBank/EMBL accession numbers AF331709 and AY289641, respectively) genes were acquired from NCBI.

Real-time quantitative PCR analysis

The primers designed for real-time quantitative PCR and optimized reaction conditions are given in Table 1. Real-time quantitative PCR was performed in the Rotor-Gene™ 6000 real-time analyzer (Corbett Research, Mortlake, Australia) using the FastStart Universal SYBR Green Master kit (ROX, Roche Ltd, Mannheim, Germany) according to the manufacturer's instructions. Reaction conditions (10 µl volumes) were optimized by changing the primer concentration and annealing temperature to minimize primer–dimer formation and to increase PCR efficiency. The following PCR profile was used: 95 °C for 5 min, 40 cycles at 95 °C for 30 s, the appropriate annealing temperature (Table 1) for 30 s and 72 °C for 30 s, followed by recording of a melting curve. The lack of primer dimmer or non-specific product accumulation was checked by melt-curve analysis. Each run included standard dilutions and negative reaction controls. The *18S* rRNA was used as a housekeeping gene, measured in parallel for each sample. The mRNA expression level of genes was expressed as the normalized ratio using the $\Delta\Delta C_t$ method according to Livak and Schmittgen (2001). The C_t values of each target gene were calculated by Rotor-Gene 6000 Application Software (Version 1.7), and the ΔC_t value of the *18S* rRNA gene was treated as an arbitrary constant for analyzing the $\Delta\Delta C_t$ value of samples. Three independent pools for each target gene were averaged, and the standard error of the mean was recorded.

Statistical analysis

Each experiment was repeated at least three times. Values in figures and tables were expressed as means ± SE. The statistical significance of the data was analyzed using a univariate analysis of variance ($P < 0.05$) (one-way ANOVA; SPSS for Windows, version 11.0).

Results

Effect of NaCl concentration on salt secretion

Salt secretion of *A. marina* grown under various concentrations of NaCl (0–600 mM), which is recognizable by salt

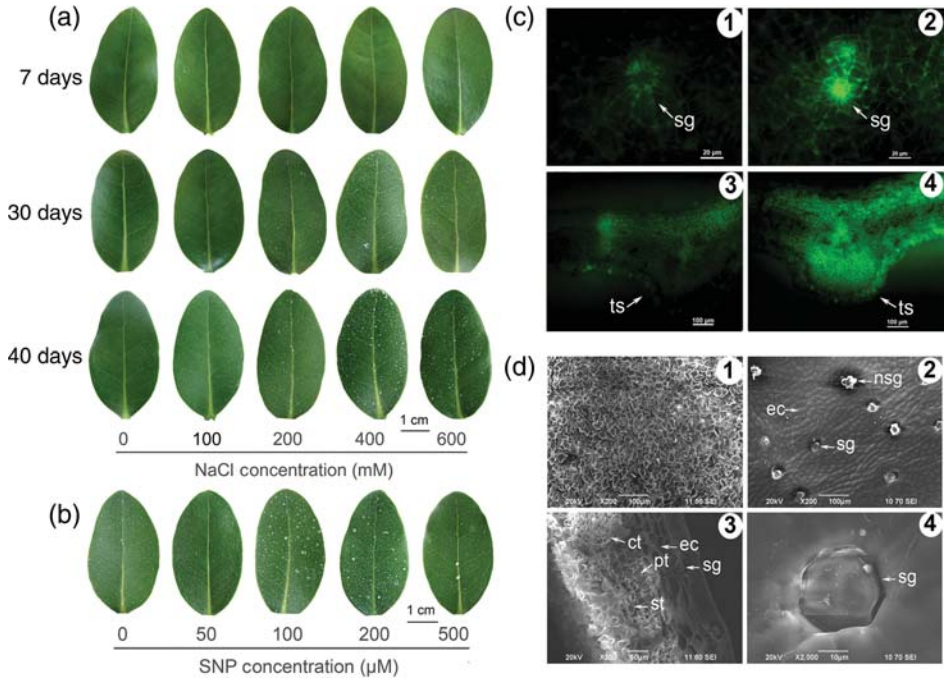

Figure 1. (a) Salt secretion on the adaxial leaf surface of *A. marina* seedlings treated with 0, 100, 200, 400 and 600 mM NaCl for 7, 30 and 40 days. (b) Salt secretion on the adaxial leaf surface of *A. marina* seedlings treated for 30 days with 0, 50, 100, 200 and 500 μM SNP addition to Hoagland solution containing 400 mM NaCl. (c) The level of endogenous NO in salt gland and transverse section of *A. marina* leaves was detected using the probe (DAF-FM DA). (1, 3) Control plant without SNP; (2, 4) plant treated with 100 μM SNP. (d) Scanning electron microscopy micrographs of abaxial surface (1), adaxial surface (2), transverse section (3) and salt glands on adaxial surface (4) of the leaves of *A. marina* seedlings grown in 400 mM NaCl for 30 days. ct, conducting tissue; ec, epidermis cell; ngh, non-gland hair; pc, hypodermal cell; pt, palisade tissue; sg, salt gland; st, sponge tissue; ts, transverse section. The scale bars are shown in the figure.

crystal deposits on leaf surfaces, was observed in order to select a suitable salinity level for subsequent experiments (Figure 1a). No salt crystals were observed on leaf surfaces until 2 weeks of salt treatments. At 30 days of salt stress, salt crystals were absent in control plants (0 mM NaCl), but their density increased with the increase in salinity from 100 to 400 mM. *Avicennia marina* appeared to survive under high salinity of up to 600 mM NaCl and secrete salt with a lower crystal density than with 400 mM NaCl. By day 40, abundant salt crystals can be observed on the leaves of *A. marina*, but the amount of secreted salt may be underestimated due to the probable loss of salt crystals.

The pattern of net Na^+ flux in salt glands of *A. marina* treated with moderate (200, 400 mM) or high (600 mM) salinity for 30 days was detected using the NMT (Figure 2a and b). The low net Na^+ efflux was measured in the salt glands of control plants (0 mM NaCl), with a mean value of 0.362 nmol cm^{-2} s^{-1}. After exposure to salt treatments, the salt glands exhibited a typical enhanced and constant Na^+ efflux, although the flux oscillated during 0–180 s (Figure 2c). The net Na^+ efflux in salt glands of *A. marina* treated with medium salinity increased with the increase in NaCl concentration. The greatest net Na^+ efflux was observed under 400 mM NaCl treatment, ranging from 3.94 to 9.15 nmol cm^{-2} s^{-1}, with a mean value of 6.35 nmol cm^{-2} s^{-1}. However, Na^+ efflux under high salinity-treated (600 mM NaCl) *A. marina* salt glands, with a mean value of 2.51 nmol cm^{-2} s^{-1}, did not show a significant difference from that under 200 mM NaCl treatment (Figure 2c). Due to the prominent presence of salt crystals on leaf surfaces and the highest net Na^+ efflux in salt glands, salinity with 400 mM NaCl for 30 days was used in subsequent studies.

Effects of NO on salt secretion rate and ion content in A. marina leaves

Avicennia marina seedlings were treated with various concentrations of SNP (0–500 μM) together with the presence of 400 mM NaCl for 30 days. To confirm the role of SNP in enhancing the endogenous NO level, the endogenous NO concentration in salt gland on the upper epidermis and transverse section of *A. marina* leaves was labeled with a specific fluorescent probe (DAF-FM DA). After *A. marina* seedlings were treated with 100 μM SNP for 30 days, compared with the control (0 μM SNP), the more intense green fluorescence due to NO was observed in both the salt gland and transverse section of leaves (Figure 1c), suggesting that the increased endogenous NO in leaves was specially induced by SNP.

The effects of SNP treatments on the amount of secreted salts and their content in the leaves were correlated with the SNP concentration used. The density of salt crystals on

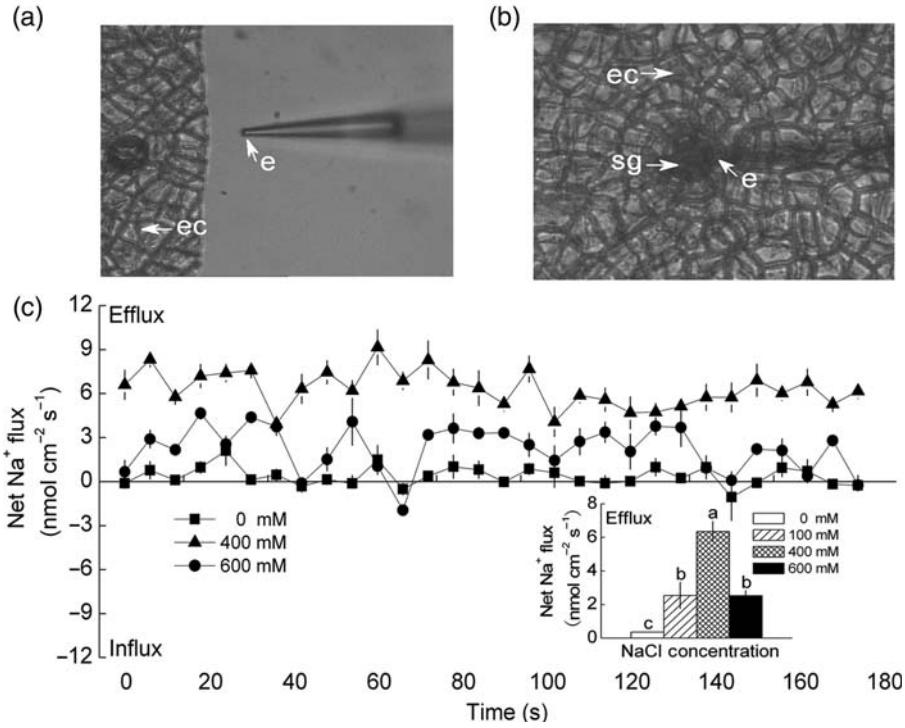

Figure 2. Net Na^+ flux from leaf salt glands of *A. marina* seedlings treated with 0, 200, 400 and 600 mM NaCl for 30 days. (a) The non-invasive ion-selective electrode was close to the adaxial side of the leaf. (b) The non-invasive ion-selective electrode was moved on the salt gland and the focal plane focuses on the leaf surface. (c) Continuous flux was recorded for 180 s from each salt gland of the upper epidermis in measuring solution (pH 6.0). Each point represents the mean of six individual salt glands, and the bars represent the standard error (SE) of the mean. The inserted section shows the mean Na^+ fluxes and SE within the measuring periods. Columns labeled with different letters (a, b and c) indicate significant differences with $P < 0.05$. e, electrode; ec, epidermis cell; sg, salt glands.

the leaves of *A. marina* treated with a medium SNP (especially at 100 μM) was highest among all the treatments (Figure 1b). Na^+ was the most abundant cation in the washing solution of leaves, comprising >96% of secreted salts (data not shown). The Na^+ secretion rate of the leaves reached a maximum (~3.8-fold higher than the control) under the 100 μM SNP treatment, and increased by 54 and 77% compared with the control at the 50 and 500 μM SNP treatments, respectively (Figure 3a). As shown in Figure 3b, the K^+ secretion rate increased by 110% of that of the control after 100 μM SNP treatment, with only 30 and 45% increase in plants treated with 50 and 500 μM SNP, respectively. The Na^+ to K^+ ratio in the washing solution was very high, and increased from 42.3 in the control to 76.4 in the 100 μM SNP-treated plants (Figure 3c). In contrast, the Na^+ to K^+ ratio in the leaves maintained a low level and reached a minimum value (only 75% of the control) under 100 μM SNP treatment, although the Na^+ content of the leaves slightly increased with the increase in SNP concentration (Figure 4a–c). On the basis of the above results, 100 μM SNP was used in other NO-related experiments.

To clarify the role of NO in inducing high Na^+ secretion rate and maintaining low Na^+ to K^+ ratio in leaves, specific NO synthesis inhibitors (*N*-nitro-L-arginine (L-NAA) as a nitric oxide synthase (NOS) inhibitor and tungstate as a nitrate reductase (NR) inhibitor) and an NO scavenger ((2-4-carboxyphenyl)-4,4,5,5-tetramethylimidazoline-1-oxyl-3-oxide, cPTIO) were used. The inhibitors and NO scavenger significantly reduced the Na^+ secretion rate and enhanced the Na^+ content in leaves (Figures 3d and 4d), resulting in abundant Na^+ accumulation in the cytosol of the cells under high salinity. These results suggest that NO plays an important role in regulating ion homeostasis in *A. marina* leaves.

Effects of NO on element ratios and ion distribution in A. marina leaves

To further investigate the effects of NO on salt secretion and ion distribution, the element ratios in the abaxial surface, adaxial surface and the transverse section of *A. marina* leaves were examined using X-ray microanalysis. The micrographs show remarkable morphological differences between the two leaf surfaces. The abaxial surface was densely covered with abundant non-gland hairs, whereas on the adaxial surface, there appeared to be few non-gland hairs, but numerous salt glands embedded in the epidermal cells (Figure 1d).

After the plants were treated with 400 mM NaCl and various concentrations of SNP (0–500 μM) for 30 days, the

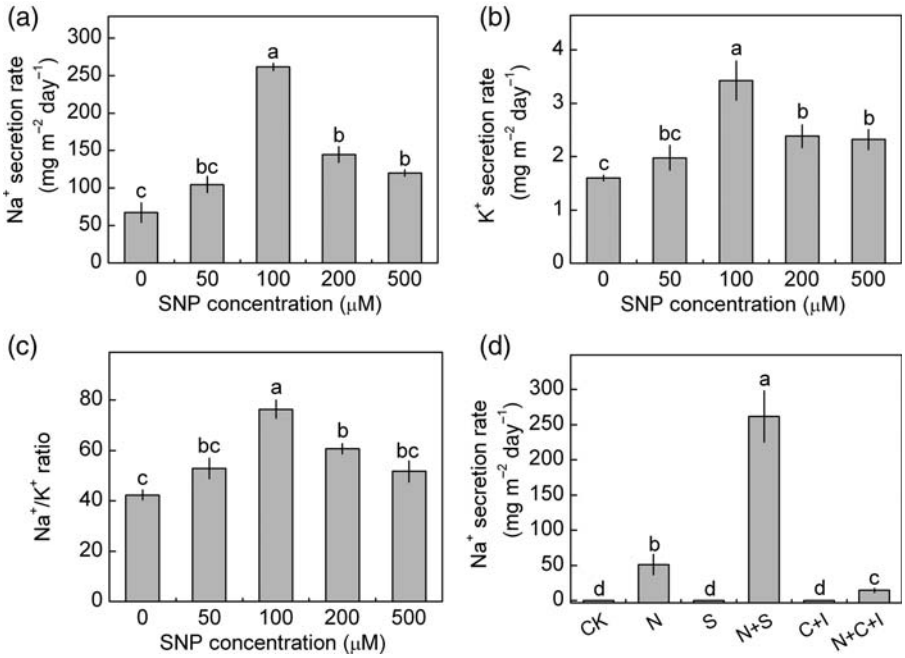

Figure 3. Effects of various concentrations of SNP on Na^+ secretion rate (a), K^+ secretion rate (b) and Na^+ to K^+ ratio (c) by the leaves of *A. marina* seedlings grown in 400 mM NaCl for 30 days. Na^+ secretion rate of *A. marina* treated with 0 mM NaCl (CK), 400 mM NaCl (N), 100 μM SNP (S), 400 mM NaCl + 100 μM SNP (N + S), 200 μM cPTIO + 100 μM L-NAA + 200 μM tungstate (C + I) and 400 mM NaCl + 200 μM cPTIO + 100 μM L-NAA + 200 μM tungstate (N + C + I) for 30 days was shown in (d). Data are mean values ± SE of four independent experiments. Columns labeled with the same letter indicate that they are not significantly different at the level of $P = 0.05$ according to one-way ANOVA.

upper second leaves were used for element ratio measurements (Table 2). A medium concentration of SNP (50, 100 or 200 μM) led to a marked increase in the Na^+ percentage and a decrease in the K^+ percentage, resulting in an increase in the Na^+ to K^+ ratio in different measured regions of the leaf surfaces. Compared with the control (0 μM SNP), the changes in percentages of Na^+, K^+ and the Na^+ to K^+ ratio were most evident in plants treated with 100 μM SNP. For instance, the Na^+ percentage increased by 36 and 27% in the non-gland hairs of the abaxial and adaxial surfaces, respectively, and the K^+ percentage decreased by 40 and 35%, respectively. Accordingly, the Na^+ to K^+ ratio increased by 124 and 97% in the non-gland hairs of the abaxial and adaxial surfaces, respectively. Remarkably, in the measured regions of the salt glands, the Na^+ percentage reached its maximum (55% higher than that of control) while the K^+ percentage reached the minimum (45% lower than that of control), leading to the greatest increase in the Na^+ to K^+ ratio by 6.44 ± 0.22, which was 182% higher than that of control under 100 μM SNP treatment.

In contrast to the leaf surfaces, the Na^+ percentage and the Na^+ to K^+ ratio in the transverse section were relatively low (Table 2). The Na^+ to K^+ ratio in hypodermal cell layers was evidently higher than that in mesophyll cells. Following 100 μM SNP treatment, the Na^+ percentage in the mesophyll cells reduced by 19% of the control and the Na^+ to K^+ ratio reached a minimum by 0.62 ± 0.09, which was 17% lower than that of control. As stated above, SNP seemed to be effective in arresting excess Na^+ accumulation in mesophyll cells under high salinity, through secreting Na^+ in salt glands and sequestrating Na^+ into the hypodermal cell layers of the leaves.

Effects of NO and inhibitors on Na^+ fluxes in salt glands of A. marina upper epidermis

To further elucidate the correlation between NO and salt secretion of salt glands, we measured the effects of SNP on Na^+ flux in the salt glands of *A. marina* upper epidermis. After being treated with 400 mM NaCl and various concentrations of SNP (0–500 μM) for 30 days, the stable and constant Na^+ efflux in the salt glands were measured using the NMT (Figure 5a). Compared with the control (0 μM SNP), accelerated Na^+ efflux was observed in the salt glands of the 100 μM SNP-treated *A. marina*, ranging from 8.47 to 16.01 nmol cm^{-2} s^{-1} and with a mean value of 11.14 nmol cm^{-2} s^{-1}. The net Na^+ efflux in the salt glands of the 200 μM SNP-treated *A. marina* has no significant difference from the control, with a mean value of 7.68 nmol cm^{-2} s^{-1}. However, the net Na^+ efflux was reduced by 65% compared with the control, after the plants were treated with 500 μM SNP for 30 days.

Na^+ kinetics in salt glands of *A. marina* grown in 400 mM NaCl for 30 days and its response to transient SNP treatment (30 μM) are shown in Figure 5b. After the addition of 30 μM SNP, the Na^+ flux remarkably drifted

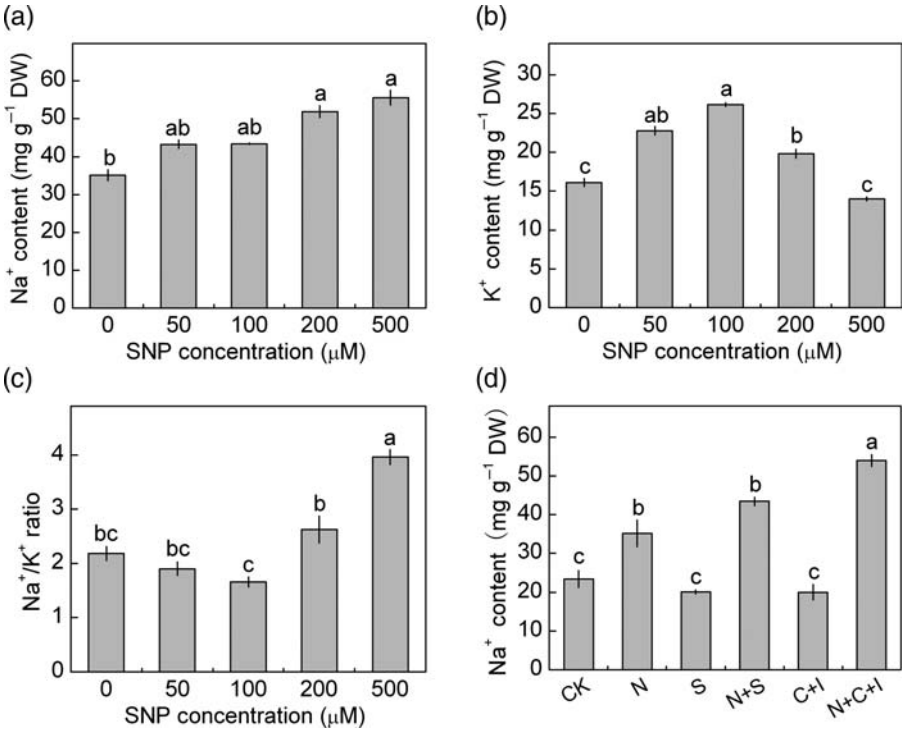

Figure 4. Effects of various concentrations of SNP on the Na^+ content (a), K^+ content (b) and Na^+ to K^+ ratio (c) in leaves of *A.marina* seedlings under 400 mM NaCl treatment for 30 days. Shown in (d) are Na^+ content of leaves of *A. marina* treated for 30 days with the following solutions: 0 mM NaCl (CK), 400 mM NaCl (N), 100 μM SNP (S), 400 mM NaCl + 100 μM SNP (N + S), 200 μM cPTIO + 100 μM L-NAA + 200 μM tungstate (C + I) and 400 mM NaCl + 200 μM cPTIO + 100 μM L-NAA + 200 μM tungstate (N + C + I). Data are mean values ± SE of four independent experiments. Columns labeled with the same letter indicate that they are not significantly different at the level of $P = 0.05$ according to one-way ANOVA.

toward the highest efflux (11.5 nmol cm^{-2} s^{-1}), lasted for 4.1–6.0 min, then finally maintained a steady level with a mean value of 8.84 nmol cm^{-2} s^{-1}. The mean net Na^+ efflux in the salt glands induced by transient SNP addition increased by 48% of the control (the mean value of Na^+ flux before SNP addition; Figure 5b).

Endogenous NO can be produced by the NR or NOS pathway in plants (Wilson et al. 2008). Specific inhibitors of NR (tungstate, 200 μM) or NOS (L-NAA, 100 μM) significantly decreased Na^+ efflux in salt glands (Figure 6a and b). After tungstate addition, the mean value of net Na^+ efflux decreased by 29% compared with the control (the mean value of Na^+ flux before inhibitor addition). Na^+ efflux was also reduced by L-NAA addition and reached a mean value of 3.58 nmol cm^{-2} s^{-1}, which was 42% lower than that of the control. These results indicate that net Na^+ efflux was specifically affected by NO. Similarly, vanadate, a specific inhibitor of PM H^+-ATPase, and amiloride, a specific inhibitor of Na^+/H^+ antiporter, significantly reduced Na^+ efflux in the salt glands of NaCl-treated *A. marina* (Figure 6c and d).

Western blot analysis of protein expression of H^+-ATPase and Na^+/H^+ antiporter affected by NO

To clarify the mechanism of enhanced Na^+ efflux and Na^+ sequestration by NO, the effects of NO on translational expression of H^+-ATPase and Na^+/H^+ antiporter were analyzed by western blot. The equal amounts of proteins, extracted from the plants treated with 400 mM NaCl and various concentrations of SNP (0–500 μM) for 30 days, were loaded in the acrylamide gels for analyzing PM H^+-ATPase and vacuolar Na^+/H^+ antiporter expressions. The changes in protein quantity were correlated with the activities of PM H^+-ATPase and vacuolar Na^+/H^+ antiporter (NHE-1). As shown in Figure 7, after quantification and normalization to β-actin, protein expression levels of both PM H^+-ATPase and NHE-1 in 100 μM SNP-treated plants reached maximum values, which were 11.17-and 1.84-fold higher than those of the respective controls (0 μM SNP). The NO-stimulated increases in Na^+ secretion in the salt glands and Na^+ sequestration possibly are involved in the enhanced protein expression of PM H^+-ATPase and NHE-1 in NaCl-treated *A. marina*.

Real-time quantitative PCR analysis of the transcriptional expression of HA1, VHA-c1, SOS1 and NHX1 genes affected by NO

To further investigate the molecular mechanism of the effects of NO on enhancing salt secretion and Na^+ sequestration in *A. marina*, the transcriptional expression of PM H^+-ATPases (*HA1*), vacuolar H^+-ATPase subunit c

Table 2. Effects of various concentrations of SNP on the percentage of Na^+, K^+ and Na^+ to K^+ ratio in abaxial surface, adaxial surface and transverse section of leaves of *A. marina* seedlings grown in 400 mM NaCl for 30 days.

Measuring region of leaf			SNP concentration (μM)				
			0	50	100	200	500
Abaxial surface	Non-gland hairs	Na^+	32.89 ± 0.85c	33.86 ± 3.78bc	44.70 ± 1.13a	35.12 ± 0.86b	30.32 ± 0.75c
		K^+	18.82 ± 1.40ab	16.07 ± 3.12b	11.36 ± 0.51c	10.24 ± 1.43c	21.48 ± 3.36a
		Na^+/K^+	1.75 ± 0.25bc	2.11 ± 0.14b	3.93 ± 0.32a	3.43 ± 0.15a	1.41 ± 0.09c
Adaxial surface	Epidermis cells	Na^+	43.14 ± 0.89c	50.85 ± 0.75b	58.41 ± 1.58a	57.41 ± 1.61a	42.95 ± 1.69c
		K^+	18.38 ± 1.20b	17.75 ± 0.92b	14.92 ± 1.14c	17.56 ± 0.90b	23.18 ± 1.40a
		Na^+/K^+	2.35 ± 0.19bc	2.87 ± 0.09b	3.91 ± 0.07a	3.25 ± 0.29ab	1.85 ± 0.15c
	Salt glands	Na^+	41.48 ± 1.52c	52.74 ± 3.18b	64.38 ± 1.84a	62.03 ± 1.42a	50.05 ± 1.15b
		K^+	18.18 ± 1.24a	16.35 ± 1.16ab	10.00 ± 1.45c	15.12 ± 1.55b	19.35 ± 1.77a
		Na^+/K^+	2.28 ± 0.21c	3.23 ± 0.32bc	6.44 ± 0.22a	4.10 ± 0.16b	2.59 ± 0.09c
	Non-gland hairs	Na^+	41.29 ± 0.99b	44.33 ± 1.93b	54.76 ± 1.27a	52.57 ± 1.45a	44.65 ± 2.49b
		K^+	24.82 ± 1.29ab	28.49 ± 0.99a	21.33 ± 2.63b	16.02 ± 0.95c	25.70 ± 3.65ab
		Na^+/K^+	1.66 ± 0.05c	1.56 ± 0.06c	2.57 ± 0.20b	3.28 ± 0.12a	1.74 ± 0.21c
Transverse section	Hypodermal cells	Na^+	18.15 ± 1.99c	18.39 ± 0.78c	31.23 ± 1.82b	21.20 ± 0.68c	40.58±1.87a
		K^+	24.59 ± 2.24a	19.95 ± 1.34b	16.96 ± 1.61bc	13.47 ± 1.12c	18.43 ± 2.12b
		Na^+/K^+	0.74 ± 0.06c	0.92 ± 0.10c	1.84 ± 0.12ab	1.57 ± 0.07b	2.20 ± 0.11a
	Mesophyll cells	Na^+	25.22 ± 2.47b	25.71 ± 3.37b	20.40 ± 1.08c	22.89 ± 1.33bc	43.57 ± 2.60a
		K^+	33.68 ± 1.40a	34.79 ± 2.44a	32.90 ± 0.87a	30.42 ± 2.32b	28.43 ± 1.40c
		Na^+/K^+	0.75 ± 0.12b	0.74 ± 0.11b	0.62 ± 0.09c	0.75 ± 0.10b	1.53 ± 0.21a

Data are means of 10–15 measurements. Values followed by the same letter in a line are not significantly different ($P = 0.05$) as described by one-way ANOVA. X-ray microanalysis was used to detect the ratio of elements in leaves. The results were expressed by the percentage of atomic number for a particular element (Na^+ or K^+) in the total atomic number for all the elements (Na^+, K^+, Ca^{2+}, Mg^{2+}, $Al^{3+}$and Mn^{2+}) measured in a given region.

(*VHA-c1*), PM Na^+/H^+ antiporter (*SOS1*) and vacuolar Na^+/H^+ antiporter (*NHX1*) in *A. marina* seedling leaves was analyzed using real-time quantitative PCR. By using RT–PCR and degenerated primers corresponding to conserved sequences of HA1, SOS1 or NHX1-like protein from other plant species (as shown in Table 1), a partial cDNA fragment of *HA1*, *SOS1* or *NHX1* was isolated from *A. marina* leaves, respectively. The deduced sequence of *A. marina* *HA1*, *SOS1* or *NHX1* has high identity (>70%) to that of *HA1*, *SOS1* or *NHX1* in other plant species. The full-length cDNA sequence of *VHA-c1* was acquired from NCBI (http://www.ncbi.nlm.nih.gov/).

Real-time quantitative PCR, with the optimized primer pairs and reaction conditions as shown in Table 1, was used to quantify the mRNA levels of *HA1*, *VHA-c1*, *SOS1* and *NHX1*. The expressions of four genes were normalized using the *18S* rRNA as internal reference gene. Figure 8 shows the relative transcript abundance of *HA1*, *VHA-c1*, *SOS1* and *NHX1* mRNA accumulation in leaves of *A. marina* grown in NaCl (400 mM) and various concentrations of SNP (0–500 μM) for 30 days. The transcripts of *HA1* and *VHA-c1* in 100 μM SNP-treated plants were more abundant than in other treatments and were increased by 138 and 54% when compared with the control (0 μM SNP), respectively. Similarly, the relative transcript abundance of *SOS1* and *NHX1* genes reached the maximum in 100 μM SNP-treated plants, which were 6.43- and 5.85-fold higher than that of the controls, respectively. However, inhibition of NO accumulation by tungstate, L-NAA and cPTIO resulted in a significant reduction in *HA1*, *VHA-c1*, *SOS1* and *NHX1* expression, and reversed the effects of NO (Figure 9).

Discussion

In some halophytes, salt secretion by specific glands scattered on the leaf surface represents an avoidance strategy that permits the regulation of intracellular ionic homeostasis after prolonged salt exposure (Barhomi et al. 2007). Salt secretion by salt glands in NaCl-treated *A. marina*, as well as other salt-secreting mangrove species, prevents excess Na^+ accumulation and maintains an optimal Na^+ to K^+ ratio in leaves (Sobrado 2002, Parida and Jha 2010). In the present study, Na^+ accounted for >96% of the secreted cation on the leaves, and crystal deposition on the leaves and net Na^+ efflux in salt glands were positively correlated with the NaCl concentration, especially with moderate salinity treatments (Figures 1a and 2c), which are in accordance with the data obtained previously by Sobrado and Greaves (2000), Sobrado (2001) and Barhomi et al. (2007). These results indicate that the salt secretion mechanism of *A. marina*, like other salt secreting species, is characterized by high selectivity in favor of Na^+ and is subject to induction in response to external NaCl concentration (Lüttge 1971, Pollak and Waisel 1979).

NO as a signaling molecule is involved in multiple resistant responses to environment stresses (Zhao et al. 2004,

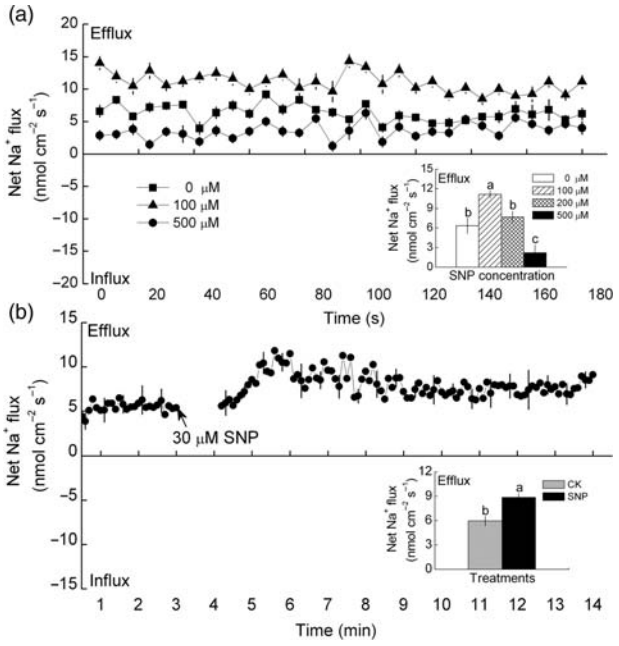

Figure 5. Effects of SNP on net Na^+ flux in leaf salt glands of *A. marina* seedlings. (a) The effects of long-term SNP treatments (0, 100, 200 and 500 μM for 30 days) on net Na^+ flux from leaf salt glands of *A. marina* seedlings grown in 400 mM NaCl. (b) The transient effect of SNP (30 μM) on Na^+ flux from the leaf salt glands of 400 mM NaCl-treated *A. marina* seedlings. Prior to SNP addition, steady Na^+ fluxes from salt glands were examined for ~3 min. Each point represents the mean of six individual salt glands, and the bars represent the SE of the mean. The inserts show mean Na^+ fluxes and SE within the measuring periods. Columns labeled with different letters (a, b and c) indicate that the changes are significantly different at $P < 0.05$.

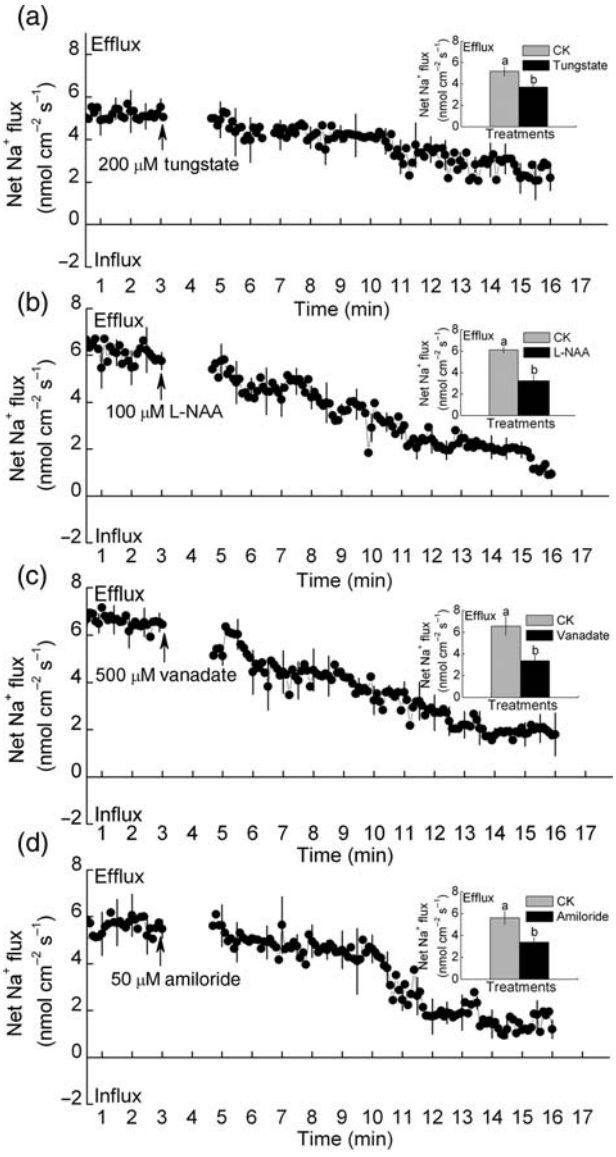

Figure 6. Continuous Na^+ flux was recorded for 16 min from leaf salt glands of *A. marina* seedlings grown in 400 mM NaCl for 30 days with the indicated inhibitor. (a) 200 μM tungstate, (b) 100 μM L-NAA, (c) 500 μM sodium orthovanadate and (d) 50 μM amiloride. Each point represents the mean of six individual salt glands and the bars represent the SE of the mean. Prior to the inhibitor shock, steady Na^+ flux was measured for ~3 min. Accordingly, the mean Na^+ flux within the measuring periods was shown in the inserted section. Columns labeled with different letters (a and b) are significantly different at $P < 0.05$.

Zhang et al. 2007, Tossi et al. 2009, Zheng et al. 2009). It has been reported that salt stress can induce a transient increase in the NO level in plants, and NO is involved in plant salt resistance by modulating ion homeostasis (Zhao et al. 2004, 2007, Zhang et al. 2006). In this study, the application of SNP at medium concentrations (such as 100 μM) significantly enhanced the Na^+ secretion rate, Na^+ percentage and Na^+ to K^+ ratio in the region of the salt gland, thus maintaining intracellular ionic homeostasis in the leaves, whereas inhibition of NO synthesis and the NO scavenger reversed the effects of SNP on the Na^+ to K^+ ratio (Figures 3 and 4 and Table 2). Moreover, using a novel NMT, both long-term and transient SNP treatments induced increases in net Na^+ efflux in the salt glands, while NO synthesis inhibitor reduced net Na^+ efflux (Figures 5 and 6a and b). From these results, we conclude that NO may participate in salt secretion for maintaining ion homeostasis to thus confer plant salt resistance. However, NO has been proved to have a dual role, either toxic or protective. The protective role of NO during osmotic stress or as a secondary messenger is in a dosage-dependent manner (Beligni and Lamattina 1999, Kopyra and Gwozdz 2003). At high NO-donor concentrations (≥500 μM SNP), when NO combined with low amounts of superoxide anion (O_2^-), the formation of peroxynitrite ($ONOO^-$) was reported to be deleterious to lipids, proteins and DNA (Lipton et al. 1993). This may explain our observation that high concentration SNP (500 μM) might not contribute much to maintaining a lower Na^+ to K^+ ratio in *A. marina* leaves.

PM H^+-ATPase (HA), a proton pump in plants encoded by a multigene family, belongs to a kind of P-type ATPase, which has a catalytic subunit of ~100 kD (Serrano 1989).

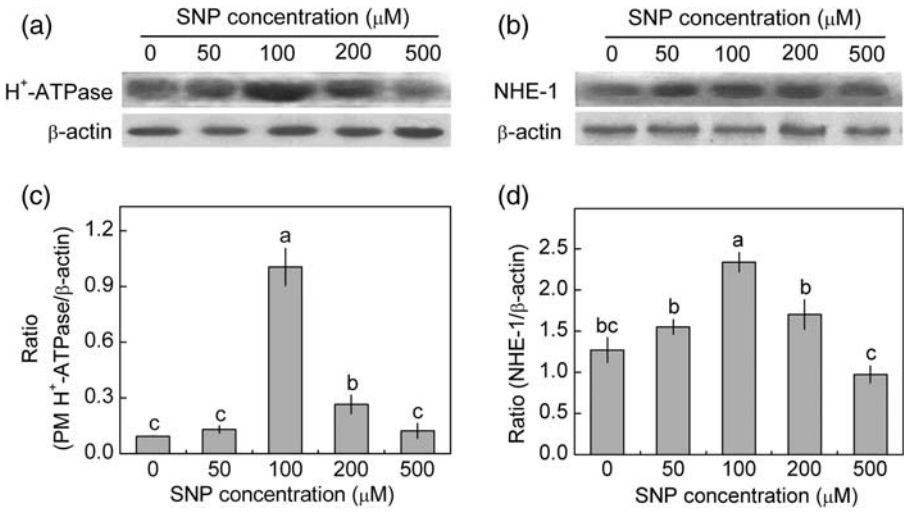

Figure 7. Western blot analysis of leaf PM H^+-ATPase (a) and vacuolar Na^+/H^+ antiporter (NHE-1) (b) of *A. marina* seedlings treated with 400 mM NaCl and various SNP concentrations for 30 days. Four independent experiments were conducted, and the immunoblotting results show similar trends of protein expression. The relative protein expression level is shown as the ratio of PM H^+-ATPase to β-actin (c) and NHE-1 to β-actin (d) analyzed with Quantity One software. Mean values ± SE were calculated from four independent experiments, and columns labeled with different letters (a, b and c) are significantly different at $P < 0.05$.

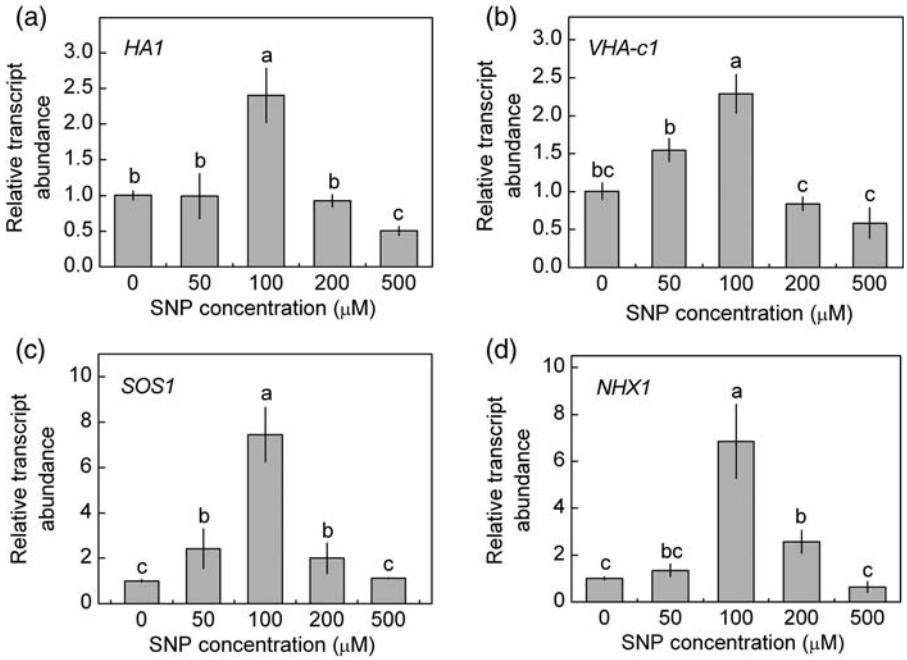

Figure 8. Real-time quantitative PCR analysis of relative transcript abundance of *HA1* (a), *VHA-c1* (b), *SOS1* (c) and *NHX1* (d) mRNA accumulation in leaves of *A. marina* seedlings treated with NaCl (400 mM) and various SNP concentrations for 30 days. Transcriptional expression of the four genes was performed by normalization with a reference gene (*18S* rRNA). Mean values ± SE were calculated from three independent experiments. Different letters (a, b and c) indicate significant differences in mRNA levels at different SNP concentrations ($P < 0.05$).

PM H^+-ATPase establishes a proton gradient that gives rise to an electrochemical gradient and pH difference across the membrane used by cross-membrane ion transporters that move their substrates against a concentration gradient (Niu et al. 1993). The force for maintaining an active Na^+/H^+ antiport in the PM is offered by the PM H^+-ATPase (Serrano 1989). In plants, Na^+/H^+ antiporter in the PM is critical for growth under high salinity as it removes the toxic Na^+ from the cytoplasm (Shi et al. 2003). *SOS1* from *Arabidopsis* is the first PM Na^+/H^+ antiporter gene cloned in higher plants (Shi et al. 2000). Recently, several *SOS1* genes have been cloned in plants, such as *OsNHA1* and

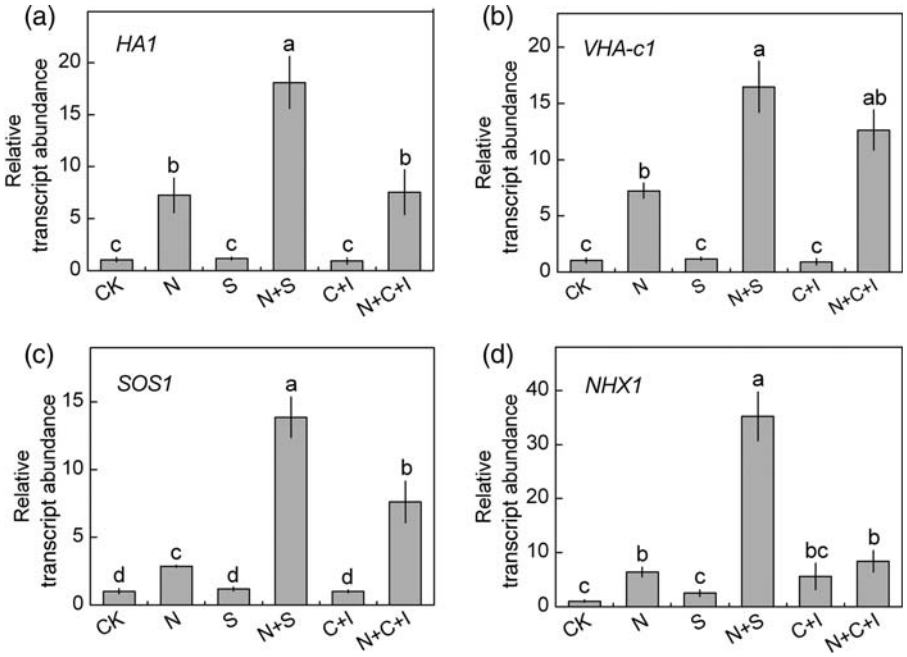

Figure 9. Real-time quantitative PCR analysis of relative transcript abundance of *HA1* (a), *VHA-c1* (b), *SOS1* (c) and *NHX1* (d) mRNA accumulation in the leaves of *A. marina* seedlings treated for 30 days with the following solutions: 0 mM NaCl (CK), 400 mM NaCl (N), 100 μM SNP (S), 400 mM NaCl + 100 μM SNP (N + S), 200 μM cPTIO + 100 μM L-NAA + 200 μM tungstate (C + I) and 400 mM NaCl + 200 μM cPTIO + 100 μM L-NAA + 200 μM tungstate (N + C + I). Transcriptional expression of the four genes was performed by normalization with a reference gene (*18S* rRNA). Mean values ± SE were calculated from three independent experiments. Different letters (a, b and c) indicate significant differences in mRNA abundance for different treatments ($P < 0.05$).

OsSOS1 from rice (Zhou et al. 2006, Martinez-Atienza et al. 2007), *PhaNHA1s* from reed (Takahashi et al. 2009), *PeNhaD1* (Ottow et al. 2005) and *PeSOS1* from poplar (Wu et al. 2007), and *CnSOS1A* and *CnSOS1B* from seagrass (Garciadeblas et al. 2007). The overexpression of *SOS1* in transgenic plants significantly improved salt tolerance in *Arabidopsis*, and mutant plants lacking SOS1 protein were extremely sensitive to salt stress (Zhu et al. 1998, Shi et al. 2003).

The activities of H^+-ATPase and Na^+/H^+ antiporter are key indexes of plant adaptations to salt stress (Niu et al. 1993, Michelet and Boutry 1995). Salt stress has been reported to increase the activities of PM H^+-ATPase and Na^+/H^+ antiporter (Zhang et al. 2006). The relative transcript abundance of *HA1* and *SOS1* mRNA in *A. marina* leaves significantly increased after prolonged exposure to moderate salinity (our unpublished data), which presumably contributes to Na^+ transport in the PM and may further modulate the cytosolic ion homeostasis.

Previous studies have showed that NO is involved in the regulation of H^+-ATPase activity under salt stress (Zhang et al. 2006). The up-regulation of PM H^+-ATPase activity has been suggested to facilitate Na^+ efflux into the apoplast, thus mitigating Na^+ toxicity to plants growing under saline conditions (Zhao et al. 2004, Zhang et al. 2006). In the present study, 100 μM SNP application remarkably enhanced the amount of PM H^+-ATPase and the transcriptional levels of *HA1* and *SOS1* genes in *A. marina* leaves (Figures 7 and 8). While NO synthesis inhibitors and NO scavenger reduced the expression of *HA1*, *SOS1*, *NHX1* and *VHA-c1* genes (Figure 9). On the basis of these observations, we suggest that NO induced both transcriptional and translational expression of the PM-located H^+-ATPase and Na^+/H^+ antiporter, thus resulting in increased Na^+ secretion in the salt glands.

Furthermore, besides detoxifying the cytoplasm by the increase in salt secretion in *A. marina*, vacuolar Na^+ sequestration is an important and cost-effective strategy for osmotic adjustment that also reduces the Na^+ concentration in the cytosol (Silva et al. 2010). Na^+ sequestration into the vacuoles depends on the expression and activity of Na^+/H^+ antiporters and H^+-ATPase in the vacuolar membrane (Shi and Zhu 2002). The vacuolar membrane H^+-ATPase generates the necessary proton gradient required for activity of Na^+/H^+ antiporter (Rea and Poole 1985, 1993). Previous studies showed that salt accumulation in mangroves occurred with Na^+ sequestration into the vacuoles of the hypodermal storage tissue (Werner and Stelzer 1990, Aziz and Khan 2001, Kura-Hotta et al. 2001, Mimura et al. 2003). In the present study, we observed a significant increase in the percentage of Na^+ in the epidermis and hypodermal cells of *A. marina* leaves after moderate SNP treatment (Table 2), suggesting that NO is involved in the enhancement of Na^+ sequestration. Moreover, the results of the real-time quantitative PCR indicated that NO significantly enhanced the mRNA accumulation of *VHA-c1* and

NHX1 genes, resulting in increased Na^+ sequestration into the vacuoles (especially in the epidermis and hypodermal cells), and further modulating ion homeostasis to cope with high salinity.

In conclusion, our results provide the first evidence, to our knowledge, that NO plays a role in enhancing salt tolerance of *A. marina* by increasing salt secretion and net Na^+ efflux in salt glands through increased expression of the *HA1* and *SOS1* genes. Moreover, NO could induce increased Na^+ sequestration into the vacuoles of the epidermis and hypodermal cells via increasing the expression of *VHA-c1* and *NHX1* genes. NO-modulated activity of H^+-ATPase and Na^+/H^+ antiporter is closely correlated with the salt resistance of the mangrove plant, *A. marina*. Further investigations are needed to decipher the potential mechanisms underlying NO-modulated gene expression in controlling salt tolerance.

Acknowledgments

We are grateful to Ting-Wu Liu and Wen-Hua Wang for assistance in experiments and Mr Thadee Vuguziga and Mr Sieh Sorie Kargbo for critically editing the manuscript. We thank Juan Sun from Xuyue Sci. and Tech. Corp., Ltd for her professional advice and technical support in Na^+ flux measurements using non-invasive micro-test technology.

Funding

This study was financially supported by the Natural Science Foundation of China (NSFC) (30930076, 30770192, 30670317, 30271065 and 39970438), the Foundation of the Chinese Ministry of Education (209084), the Program for New Century Excellent Talents in Xiamen University (NCETXMU X07115) to H.Z. and a Changjiang Scholarship (X09111) to P.Z.

References

Apse, M.P., G.S. Aharon, W.A. Snedden and E. Blumwald. 1999. Salt tolerance conferred by overexpression of a vacuolar Na^+/H^+ antiport in *Arabidopsis*. Science 285:1256–1258.

Aziz, I. and M.A. Khan. 2001. Effect of seawater on the growth, ion content and water potential of *Rhizophora mucronata* Lam. J. Plant Res. 114:369–373.

Balsamo, R.A., M.E. Adams and W.W. Thomson. 1995. Electrophysiology of the salt glands of *Avicennia germinans*. Int. J. Plant Sci. 156:658–667.

Barhomi, Z., W. Djebali, A. Smaoui, W. Chaibi and C. Abdelly. 2007. Contribution of NaCl excretion to salt resistance of *Aeluropus littoralis* (Willd) Parl. J. Plant Physiol. 164:842–850.

Beligni, M.V. and L. Lamattina. 1999. Nitric oxide counteracts cytotoxic processes mediated by reactive oxygen species in plant tissues. Planta 208:337–344.

Beligni, M.V. and L. Lamattina. 2002. Nitric oxide interferes with plant photo-oxidative stress by detoxifying reactive oxygen species. Plant Cell Environ. 25:737–748.

Blumwald, E. 2000. Sodium transport and salt tolerance in plants. Curr. Opin. Cell Biol. 12:431–434.

Boon, P.I. and W.G. Allaway. 1986. Rates of ionic specificity of salt secretion from excised leaves of the mangrove, *Avicennia marina* (Forsk.) Vierh. Aquat. Bot. 26:143–153.

Bradford, M.M. 1976. A rapid and sensitive method for the quantitation of microgram quantities of protein utilizing the principle of protein-dye binding. Anal. Biochem. 72:248–254.

Chauhan, S., N. Forsthoefel, Y.Q. Ran, F. Quigley, D.E. Nelson and H.J. Bohnert. 2000. Na^+/myo-inositol symporters and Na^+/H^+-antiport in *Mesembryanthemum crystallinum*. Plant J. 24:511–522.

Chen, M., J. Song and B.S. Wang. 2010. NaCl increases the activity of the plasma membrane H^+-ATPase in C-3 halophyte *Suaeda salsa* callus. Acta. Physiol. Plant 32:27–36.

Chen, Z.H., I.I. Pottosin, T.A. Cuin et al. 2007. Root plasma membrane transporters controlling K^+/Na^+ homeostasis in salt-stressed barley. Plant Physiol. 145:1714–1725.

Chinnusamy, V., A. Jagendorf and J.K. Zhu. 2005. Understanding and improving salt tolerance in plants. Crop Sci. 45:437–448.

Corpas, F.J., J.B. Barroso, A. Carreras, R. Valderrama, J.M. Palma, A.M. Léon, L.M. Sandalio and L.A. del Río. 2006. Constitutive arginine-dependent nitric oxide synthase activity in different organs of pea seedlings during plant development. Planta 224: 246–254.

Ding, F., J. Song, Y. Ruan and B.S. Wang. 2009. Comparison of the effects of NaCl and KCl at the roots on seedling growth, cell death and the size, frequency and secretion rate of salt glands in leaves of *Limonium sinense*. Acta Physiol. Plant 31:343–350.

Drennan, P. and N.W. Pammenter. 1982. Physiology of salt excretion in the mangrove *Avicennia marina* (Forsk.) Vierh. New Phytol. 91:597–606.

Dschida, W.J., K.A. Platt-Aloia and W.W. Thomson. 1992. Epidermal peels of *Avicennia germinans* (L.) Stearn: a useful system to study the function of salt glands. Ann. Bot. 70:501–509.

Duke, N.C., M.C. Ball and J.C. Ellison. 1998. Factors influencing biodiversity and distributional gradients in mangroves. Global Ecol. Biogeogr. Lett. 7:27–47.

Flowers, T.J., S.A. Flowers, M.A. Hajibagheri and A.R. Yeo. 1990. Salt tolerance in the halophytic wild rice, *Porteresia coarctata* Tateoka. New Phytol. 114:675–684.

Fukuda, A., A. Nakamura, A. Tagiri, H. Tanaka, A. Miyao, H. Hirochika and Y. Tanaka. 2004. Function, intracellular localization and the importance in salt tolerance of a vacuolar Na^+/H^+ antiporter from rice. Plant Cell Physiol. 45:146–159.

Garciadeblas, B., R. Haro and B. Benito. 2007. Cloning of two SOS1 transporters from the seagrass *Cydocea nodosamo*. SOS1 transporters from *Cymodocea* and *Arabidopsis* mediate potassium uptake in bacteria. Plant Mol. Biol. 63:479–490.

Gaxiola, R.A., R. Rao, A. Sherman, P. Grisafi, S.L. Alper and G. R. Fink. 1999. The *Arabidopsis thaliana* proton transporters, AtNhx1 and Avp1, can function in cation detoxification in yeast. Proc. Natl Acad. Sci. USA 96:1480–1485.

Hamada, A., M. Shono, T. Xia, M. Ohta, Y. Hayashi, A. Tanaka and T. Hayakawa. 2001. Isolation and characterization of a Na^+/H^+ antiporter gene from the halophyte *Atriplex gmelini*. Plant Mol. Biol. 46:35–42.

Hasegawa, P.M., R.A. Bressan, J.K. Zhu and H.J. Bohnert. 2000. Plant cellular and molecular responses to high salinity. Annu. Rev. Plant Physiol. Plant Mol. Biol. 51:463–499.

Hassidim, M., Y. Braun, H.R. Lerner and L. Reinhold. 1986. Studies on H^+ translocating ATPase in plants of varying resistance to salinity. Plant Physiol. 81:1057–1061.

He, Y.K., R.H. Tang, H. Hao et al. 2004. Nitric oxide represses the *Arabidopsis* floral transition. Science 305:1968–1971.

Kerkeb, L., J.P. Donaire, K. Venema and M.P. Rodriguez-Rosales. 2001. Tolerance to NaCl induces changes in plasma membrane lipid composition, fluidity and H^+-ATPase activity of tomato calli. Physiol. Plant. 113:217–224.

Kirsch, M., A. Zhigang, R. Viereck, R. Low and T. Rausch. 1996. Salt stress induces an increased expression of V-type H^+-ATPase in mature sugar beet leaves. Plant Mol. Biol. 32:543–547.

Kopyra, M. and E.A. Gwozdz. 2003. Nitric oxide stimulates seed germination and counteracts the inhibitory effect of heavy metals and salinity on root growth of *Lupinus luteus*. Plant Physiol. Biochem. 41:1011–1017.

Kura-Hotta, M., M. Mimura, T. Tsujimura, S. Washitani-Nemoto and T. Mimura. 2001. High salt-treatment-induced Na^+ extrusion and low salt-treatment-induced Na^+ accumulation in suspension-cultured cells of the mangrove plant, *Bruguiera sexangula*. Plant Cell Environ. 24:1105–1112.

Lehr, A., M. Kirsch, R. Viereck, J. Schiemann and T. Rausch. 1999. cDNA and genomic cloning of sugar beet V-type H^+-ATPase subunit A and c isoforms: evidence for coordinate expression during plant development and coordinate induction in response to high salinity. Plant Mol. Biol. 39:463–475.

Lipton, S.A., Y.B. Choi, Z.H. Pan, S.Z. Lei, H.S. Chen, N.J. Sucher, J. Loscalzo, D.J. Singel and J.S. Stamler. 1993. A redox-based mechanism for the neuroprotective and neurodestructive effects of nitric oxide and related nitroso-compounds. Nature 364:626–632.

Livak, K.J. and T.D. Schmittgen. 2001. Analysis of relative gene expression data using real-time quantitative PCR and the 2(T) (-Delta Delta C) method. Methods 25:402–408.

Lüttge, U.. 1971. Structure and function of plant glands. Annu. Rev. Plant Physiol. 22:23–44.

Malerba, M., N. Contran, M. Tonelli, P. Crosti and R. Cerana. 2008. Role of nitric oxide in actin depolymerization and programmed cell death induced by fusicoccin in sycamore (*Acer pseudoplatanus*) cultured cells. Physiol. Plant. 133:449–457.

Martinez-Atienza, J., X.Y. Jiang, B. Garciadeblas, I. Mendoza, J.K. Zhu, J.M. Pardo and F.J. Quintero. 2007. Conservation of the salt overly sensitive pathway in rice. Plant Physiol. 143:1001–1012.

Michelet, B. and M. Boutry. 1995. The plasma membrane H^+-ATPase: a highly regulated enzyme with multiple physiological functions. Plant Physiol. 108:1–6.

Mimura, T., M. Kura-Hotta, T. Tsujimura, M. Ohnishi, M. Miura, Y. Okazaki, M. Mimura, M. Maeshima and S. Washitani-Nemoto. 2003. Rapid increase of vacuolar volume in response to salt stress. Planta 216:397–402.

Neill, S.J., R. Desikan, A. Clarke and J.T. Hancock. 2002. Nitric oxide is a novel component of abscisic acid signaling in stomatal guard cells. Plant Physiol. 128:13–16.

Niu, X., M.L. Narasimhan, R.A. Salzman, R.A. Bressan and P.M. Hasegawa. 1993. NaCl regulation of plasma membrane H^+-ATPase gene expression in a glycophyte and a halophyte. Plant Physiol. 103:713–718.

Oh, D.H., S.Y. Lee, R.A. Bressan, D.J. Yun and H.J. Bohnert. 2010. Intracellular consequences of SOS1 deficiency during salt stress. J. Exp. Bot. 61:1205–1213.

Olias, R., Z. Eljakaoui, J. Li, P.A. De Morales, M.C. Marin-Manzano, J.M. Pardo and A. Belver. 2009. The plasma membrane Na^+/H^+ antiporter SOS1 is essential for salt tolerance in tomato and affects the partitioning of Na^+ between plant organs. Plant Cell Environ. 32:904–916.

Ottow, E.A., A. Polle, M. Brosche, J. Kangasjarvi, P. Dibrov, C. Zorb and T. Teichmann. 2005. Molecular characterization of *PeNhaD1*: the first member of the NhaD Na^+/H^+ antiporter family of plant origin. Plant Mol. Biol. 58:75–88.

Parida, A.K. and B. Jha. 2010. Salt tolerance mechanisms in mangroves: a review. Trees Struct. Funct. 24:199–217.

Pollak, G. and Y. Waisel. 1979. Ecophysiology of salt excretion in *Aeluropus littoralis* (Graminae). Plant Physiol. 47:177–84.

Quintero, F.J., M.R. Blatt and J.M. Pardo. 2000. Functional conservation between yeast and plant endosomal Na^+/H^+ antiporters. FEBS Lett. 471:224–228.

Quintero, F.J., M. Ohta, H.Z. Shi, J.K. Zhu and J.M. Pardo. 2002. Reconstitution in yeast of the *Arabidopsis* SOS signaling pathway for Na^+ homeostasis. Proc. Natl Acad. Sci. USA 99:9061–9066.

Rea, P.A. and R.J. Poole. 1985. Proton-translocating inorganic pyrophosphatase in red beet (*Beta vulgaris* L.) tonoplast vesicles. Plant Physiol. 77:46–52.

Rea, P.A. and R.J. Poole. 1993. Vacuolar H^+-translocating pyrophosphatase. Annu. Rev. Plant Physiol. Plant Mol. Biol. 44:157–180.

Rengasamy, P. 2006. World salinization with emphasis on Australia. J. Exp. Bot. 57:1017–1023.

Serrano, R. 1989. Structure and function of plasma membrane ATPase. Annu. Rev. Plant Physiol. 40:61–94.

Shi, H.Z. and J.K. Zhu. 2002. Regulation of expression of the vacuolar Na^+/H^+ antiporter gene *AtNHX1* by salt stress and abscisic acid. Plant Mol. Biol. 50:543–550.

Shi, H.Z., M. Ishitani, C.S. Kim and J.K. Zhu. 2000. The *Arabidopsis thaliana* salt tolerance gene *SOS1* encodes a putative Na^+/H^+ antiporter. Proc. Natl Acad. Sci. USA 97:6896–6901.

Shi, H.Z., B.H. Lee, S.J. Wu and J.K. Zhu. 2003. Overexpression of a plasma membrane Na^+/H^+ antiporter gene improves salt tolerance in *Arabidopsis thaliana*. Nat. Biotechnol. 21: 81–85.

Shi, Q.H., F. Ding, X.F. Wang and M. Wei. 2007. Exogenous nitric oxide protect cucumber roots against oxidative stress induced by salt stress. Plant Physiol. Biochem. 45:542–550.

Sibole, J.V., C. Cabot, W. Michalke, C. Poschenrieder and J. Barcelo. 2005. Relationship between expression of the PM H^+-ATPase, growth and ion partitioning in the leaves of salt-treated *Medicago* species. Planta 221:557–566.

Silva, P., A.R. Facanha, R.M. Tavares and H. Geros. 2010. Role of tonoplast proton pumps and Na^+/H^+ antiport system in salt tolerance of *Populus euphratica* Oliv. J. Plant Growth Regul. 29:23–34.

Sobrado, M.A. 2001. Effect of high external NaCl concentration on the osmolality of xylem sap, leaf tissue and leaf glands secretion of the mangrove *Avicennia germinans* L. Flora 196:63–70.

Sobrado, M.A. 2002. Effect of drought on leaf gland secretion of the mangrove *Avicennia germinans* L. Trees Struct. Funct. 16:1–4.

Sobrado, M.A. and E.D. Greaves. 2000. Leaf secretion composition of the mangrove species *Avicennia germinans* (L.) in relation to salinity: a case study by using total-reflection X-ray fluorescence analysis. Plant Sci. 159:1–5.

Sun, J., S.L. Chen, S.X. Dai, et al. 2009a. NaCl-induced alternations of cellular and tissue ion fluxes in roots of salt-resistant and salt-sensitive poplar species. Plant Physiol. 149:1141–1153.

Sun, J., S.X. Dai, R.G. Wang, et al. 2009b. Calcium mediates root K^+/Na^+ homeostasis in poplar species differing in salt tolerance. Tree Physiol. 29:1175–1186.

Takahashi, R., S. Liu and T. Takano. 2009. Isolation and characterization of plasma membrane Na^+/H^+ antiporter genes from salt-sensitive and salt-tolerant reed plants. J. Plant Physiol. 166:301–309.

Tossi, V., L. Lamattina and R. Cassia. 2009. An increase in the concentration of abscisic acid is critical for nitric oxide-mediated plant adaptive responses to UV-B irradiation. New Phytol. 181:871–879.

Vazquez, M.D., C. Poschenrieder, I. Corrales and J. Barcelo. 1999. Change in apoplastic aluminum during the initial growth response to aluminum by roots of a tolerant maize variety. Plant Physiol. 119:435–444.

Wendehenne, D., J. Durner and D.F. Klessig. 2004. Nitric oxide: a new player in plant signalling and defence responses. Curr. Opin. Plant Biol. 7:449–455.

Werner, A. and R. Stelzer. 1990. Physiological responses of the mangrove *Rhizophora mangle* grown in the absence and presence of NaCl. Plant Cell Environ. 13:243–255.

Wilson, I.D., S.J. Neill and J.T. Hancock 2008. Nitric oxide synthesis and signalling in plants. Plant Cell Environ. 31: 622–631.

Wu, Y., N. Ding, X. Zhao, M. Zhao, Z. Chang, J. Liu and L. Zhang. 2007. Molecular characterization of PeSOS1: the putative Na^+/H^+ antiporter of *Populus euphratica*. Plant Mol Biol. 65:1–11.

Xue, Z.Y., D.Y. Zhi, G.P. Xue, H. Zhang, Y.X. Zhao and G.M. Xia. 2004. Enhanced salt tolerance of transgenic wheat (*Tritivum aestivum* L.) expressing a vacuolar Na^+/H^+antiporter gene with improved grain yields in saline soils in the field and a reduced level of leaf Na^+. Plant Sci. 167:849–859.

Yang, Q., Z.Z. Chen, X.F. Zhou, H.B. Yin, X. Li, X.F. Xin, X.H. Hong, J.K. Zhu and Z.Z. Gong. 2009. Overexpression of *SOS* (Salt Overly Sensitive) genes increases salt tolerance in transgenic *Arabidopsis*. Mol. Plant 2:22–31.

Zhang, F., Y.P. Wang, Y.L. Yang, H. Wu, D. Wang and J.Q. Liu. 2007. Involvement of hydrogen peroxide and nitric oxide in salt resistance in the calluses from *Populus euphratica*. Plant Cell Environ. 30:775–785.

Zhang, H.X. and E. Blumwald. 2001. Transgenic salt-tolerant tomato plants accumulate salt in foliage but not in fruit. Nat. Biotechnol. 19:765–768.

Zhang, Y.Y., L.L. Wang, Y.L. Liu, Q. Zhang, Q.P. Wei and W.H. Zhang. 2006. Nitric oxide enhances salt tolerance in maize seedlings through increasing activities of proton-pump and Na^+/H^+ antiport in the tonoplast. Planta 224:545–555.

Zhao, L.Q., F. Zhang, J.K. Guo, Y.L. Yang, B.B. Li and L.X. Zhang. 2004. Nitric oxide functions as a signal in salt resistance in the calluses from two ecotypes of reed. Plant Physiol. 134:849–857.

Zhao, M.G., Q.T. Tian and W.H. Zhang. 2007. Nitric oxide synthase-dependent nitric oxide production is associated with salt tolerance in *Arabidopsis*. Plant Physiol. 144:206–217.

Zheng, C.F., D. Jiang, F.L. Liu, T.B. Dai, W.C. Liu, Q. Jing and W.X. Cao. 2009. Exogenous nitric oxide improves seed germination in wheat against mitochondrial oxidative damage induced by high salinity. Environ. Exp. Bot. 67:222–227.

Zhou, G.A., Y. Jiang, Q. Yang, J.F. Wang, J. Huang and H.S. Zhang. 2006. Isolation and characterization of a new Na^+/H^+ antiporter gene *OsNHA1* from rice (*Oryza sativa* L.). DNA Sequence 17:24–30.

Zhu, J.K.. 2002. Salt and drought stress signal transduction in plants. Annu. Rev. Plant Biol. 53:247–273.

Zhu, J.K.. 2003. Regulation of ion homeostasis under salt stress. Curr. Opin. Plant Biol. 6:441–445.

Zhu, J.K., J.P. Liu and L.M. Xiong. 1998. Genetic analysis of salt tolerance in *Arabidopsis*: evidence for a critical role of potassium nutrition. Plant Cell 10:1181–1191.